



LAWRENCE
LIVERMORE
NATIONAL
LABORATORY

Comparison of Ramsauer and Optical Model Neutron Angular Distributions

D. P. McNabb, J. D. Anderson, R. W. Bauer, F. S.
Dietrich, S. M. Grimes, C. A. Hagmann

April 20, 2004

Nuclear Science and Engineering

Disclaimer

This document was prepared as an account of work sponsored by an agency of the United States Government. Neither the United States Government nor the University of California nor any of their employees, makes any warranty, express or implied, or assumes any legal liability or responsibility for the accuracy, completeness, or usefulness of any information, apparatus, product, or process disclosed, or represents that its use would not infringe privately owned rights. Reference herein to any specific commercial product, process, or service by trade name, trademark, manufacturer, or otherwise, does not necessarily constitute or imply its endorsement, recommendation, or favoring by the United States Government or the University of California. The views and opinions of authors expressed herein do not necessarily state or reflect those of the United States Government or the University of California, and shall not be used for advertising or product endorsement purposes.

Comparison of Ramsauer and Optical Model Neutron Angular Distributions

D. P. McNabb,^{*} J. D. Anderson, R. W. Bauer, F. S. Dietrich, S. M. Grimes,⁺ C. A. Hagmann
University of California
Lawrence Livermore National Laboratory
P.O. Box 808
Livermore, CA 94551

^{*}Email Address: dpmcnabb@llnl.gov

⁺Permanent Address, Department of Physics, Ohio University, Athens, OH 45701

Abstract

In a recent paper it has been shown that the nuclear Ramsauer model does not do well in representing details of the angular distribution of neutron elastic scattering for incident energies of less than 60 MeV for ^{208}Pb . We show that the default angular bin dispersion most widely used in Monte Carlo transport codes is such that the observed differences in angular shapes are on too fine a scale to affect transport calculations. The effect of increasing the number of Monte Carlo angle bins is studied to determine the dispersion necessary for calculations to be sensitive to the observed discrepancies in angular distributions. We also show that transport calculations are sensitive to differences in the elastic scattering cross section given by recent fits of ^{208}Pb data compared with older fits.

I. Introduction

The nuclear Ramsauer model has been used for decades to explain features of the neutron total cross section results.^{1,2} When precision data³ (with typical errors of only a few percent) became available it was quite surprising that such a simple model could adequately represent these data.⁴ A theoretical investigation⁵ of this “single-phase-shift slug model” demonstrated that nuclear refraction essentially made all neutron path lengths in the nucleus equal for neutron energies from a few MeV to approximately 60 MeV. Franco⁶ had previously demonstrated that one did not need a “single phase shift” but merely that the average of the phase shifts varied smoothly with energy. Subsequently a large amount of precision neutron total cross section data⁷ was successfully fit with this model.⁸

Azam and Gowda⁹ have recently proposed a more stringent test of the Ramsauer model and have compared calculated angular distributions of elastically scattered neutrons with optical model calculations. The shape of the angular distribution derived from the Ramsauer model did not agree in detail with the angular distributions derived from the optical model except for the forward maximum. They thus correctly conclude that this simple model does not give an accurate representation of the neutron elastic scattering cross section.

The point of this article is to demonstrate that in spite of deficiencies in calculating angular distributions with the Ramsauer model, it may be adequate for Monte Carlo neutron transport calculations^{10,11,12} and may give more accurate results than using an optical model if these optical model parameters have not been carefully fit to new, high precision neutron total cross section measurements. The Ramsauer model has several practical features that make it generally useful: (1) it requires only 5-10 parameters to globally represent the total neutron cross section within 2% for nuclei between calcium and uranium over the energy range of 6 to 60 MeV, (2) it can be computed algebraically, and (3) it gives a reasonably accurate intuitive picture of the correct scaling relationships for baryon number, isospin, and incident neutron energy.

First we present a rationale as to why the elastic scattering cross sections generated with the Ramsauer model may be useful in transport calculations and outline an approach to incorporate Ramsauer model results into transport codes. We then compare the differences in fits of elastic and total cross section data over time and demonstrate that reliable fits to these data are very important to the accuracy of transport calculations. We then examine the standard angle bin structure of popular Monte Carlo neutron transport codes and demonstrate their sensitivity to elastic angular distributions. We conclude with a discussion on the applicability of the Ramsauer model and the issues to be addressed if better than 1% precision is desired in transporting elastically scattered neutrons.

II. Ramsauer Differential Elastic Scattering Distributions

From equations (3) and (6) of the paper by Azam and Gowda⁹ we obtain

$$\sigma(\theta) = \frac{\lambda^2}{4} \left| \sum_l (2l+1) (1 - e^{i\delta_l}) P_l(\cos\theta) \right|^2 \quad (1)$$

where $\sigma(\theta)$ is the differential shape-elastic cross section, l is the orbital angular momentum quantum number. The summation \sum_l over integer values of l is to be taken from $l=0$ to $l_{max} = R/\lambda = kR$ where R is the potential scattering radius, λ is the reduced wavelength of the incoming neutron, δ_l and σ_l are defined as in Ref. 5. The sharp cutoff approximation is typically employed, so that l_{max} is the integer nearest to, but less than, kR .

Camarda¹³ has suggested to us a formulation equivalent to Eq. 1 given as

$$\begin{aligned} \sigma_{el}(\theta) &= \frac{\lambda^2}{4} \left(\left(\sum_l \sigma_l \cos\theta \right)^2 + \sum_l \sigma_l^2 \sin^2\theta \right) \left[\sum_l (2l+1) P_l(\cos\theta) \right]^2 \\ &= \frac{\lambda^2}{2} \sum_l \frac{1 + \sigma_l^2}{2} \sigma_l \cos\theta \left[\sum_l (2l+1) P_l(\cos\theta) \right]^2 \end{aligned} \quad (2)$$

This expression can be integrated over angle to give the integrated elastic cross section as

$$\sigma_{el} = 2\lambda^2 \sum_l \frac{1 + \sigma_l^2}{2} \sigma_l \cos\theta \left[\sum_l (2l+1) P_l(\cos\theta) \right]^2 \quad (3)$$

Azam and Gowda⁹ also introduced a useful concept called the “relative differential shape-elastic cross section” σ_{rel} defined as

$$\sigma_{rel} \equiv \frac{\sigma_{el}(\theta)}{\sigma_{el}} = \frac{1}{4} \frac{\sum_l (2l+1) P_l(\cos\theta) \left[\sum_l (2l+1) P_l(\cos\theta) \right]^2}{\sum_l (2l+1) P_l(\cos\theta)} \quad (4)$$

The quantity σ_{rel} is typically tabulated and sampled in Monte Carlo transport codes when sourcing elastically scattered neutrons to determine the scattering angle. The energy of the elastically scattered neutron is then determined using two-body kinematics. The quantity σ_{rel} is plotted in Azam and Gowda’s Figs. 1 through 21. What we note from this comparison (Figs. 1-3

and 6-8 in their paper⁹) is that the Ramsauer model compares favorably with the optical model calculations for the forward maximum (0-20 degrees) in the elastic scattering distribution. This is not surprising since a Ramsauer model which fits the total neutron cross section also accurately (within a few percent) predicts the zero-degree elastic cross section as given by the Wick limit¹⁴ which relates the zero-degree cross section to the total cross section. The average elastic cross section is also well described (to a few percent) by the Ramsauer model since the model is able to fit the oscillations in the total cross section to the order of 1-2% and these oscillations are due to variations in the elastic cross section.⁸ However, beyond 30 degrees Azam and Gouda⁹ have demonstrated large discrepancies between angular distributions as calculated with the Ramsauer and optical models (see Figs. 12 through 21 in Ref. 9). In the Appendix a simple two-radii extension to the Ramsauer model is described which helps to alleviate the discrepancy at larger scattering angles, but this extension is not considered in the body of the paper.

From the perspective of neutron transport, small-angle elastic scattering and average elastic scattering properties are well described by the Ramsauer model for $5 < E_n < 60$ MeV. In Section IV, we also show that the average large-angle scattering, which results in neutron removal from the beam, is well described. Since these quantities are the most important features of elastic scattering for transport calculations we now demonstrate how these cross sections might be adapted for use in a neutron transport code.

However, two problems arise from using Eqs. 2-4 in transport codes both associated with discontinuities caused by using the sharp cutoff approximation for the summation in Eqs. 1 and 2. The first problem is discontinuity in the shape of the predicted angular distribution for integer l , e.g. $\sigma_{el}(\theta, kR=6.9) \neq \sigma_{el}(\theta, kR=7.0)$. The second problem is that the zero degree cross section does not extrapolate to the Wick limit except for integer values of $kR=l$.

These problems could be overcome by adding a nuclear surface to our square well potential from which we generated the Ramsauer model. A much simpler solution is to account for the cross section due to a fractional kR , by introducing a smooth interpolation between successive values of l_{max} that has been constructed to preserve Wick's limit:

$$\sigma_{el}(\theta) = \frac{\lambda^2}{2} \frac{1 + \sin^2 \theta}{2} \left[\sum_{l=0}^{l_{max}} (2l+1) P_l(\cos \theta) + ((kR+1)^2 - (l_{max}+1)^2) P_{l_{max}+1}(\cos \theta) \right]^2 \quad (5)$$

This solution gets rid of the discontinuities in the angular shape as a function of bombarding energy and correctly extrapolates to Wick's limit at zero degrees when $kR \ll 1$. This philosophy results in a slightly modified expression for the angular distribution of elastically scattered neutrons

$$\sigma = \frac{1}{4} \frac{\sum_{l=0}^{l_{\max}} (2l+1) P_l(\cos\theta) + ((kR+1)^2 \sum_{l=l_{\max}+1}^{\infty} (l_{\max}+1)^2) P_{l_{\max}+1}(\cos\theta)}{(kR+1)} \quad (6)$$

Eqs. 5 and 6 have been used in the remainder of this paper for the purposes of generating elastic scattering properties based on the Ramsauer model to compare with optical model results. Expressions for k and R were taken from Ref. 8, and for the case of ^{208}Pb were $k = 0.103$ and $R = 3.674(\sqrt{35.0 + 0.8E})/\sqrt{E}$ where E is the energy of the incident neutron.

III. Ramsauer and Optical Model Fits

For the purpose of neutron transport calculations we consider the optical model as merely a convenient way of representing a large quantity of measurements. To that end, we judge the “goodness” of each set of model parameters on their ability to fit experimental data. By this criterion we judge the recent model calculations of Koning and Delaroche¹⁵ (K&D) as the best representation of the newer, more precise total cross section measurements.⁷ We therefore take the cross sections generated by K&D as our standard for comparison, i.e., we assume K&D are a good representation of nature.

Different fits to the total, elastic, and reaction cross section data for $n + {}^{208}\text{Pb}$ are plotted in Figs. 1-3. The K&D optical model fits (circa 2003) are compared with fits by Becchetti and Greenlees¹⁶ (circa 1969) and with the Ramsauer model fit results from Ref. 8. Inspection of Fig. 1 indicates that for $n + {}^{208}\text{Pb}$ the Ramsauer model fits are significantly better at representing the total cross section data than the B&G optical model fit. In addition, for neutron energies $10 < E_n < 40$ MeV, the Ramsauer model is also better than the B&G optical model fit at representing the elastic and reaction cross sections, as shown in Figs. 2 and 3 respectively. In fairness, however, it should be noted that Becchetti and Greenlees did not have access to newer data that indicates that the imaginary potential decreases at lower neutron energies.

The Ramsauer model reproduces the angular distribution of elastically scattered neutrons near zero degrees as shown at $E_n = 14$ MeV in Fig. 4. While the Becchetti and Greenlees optical model angular distribution, shown in Fig. 5, is somewhat better at reproducing the first maximum in the forward direction, this model also does poorly at reproducing large-angle scattering.

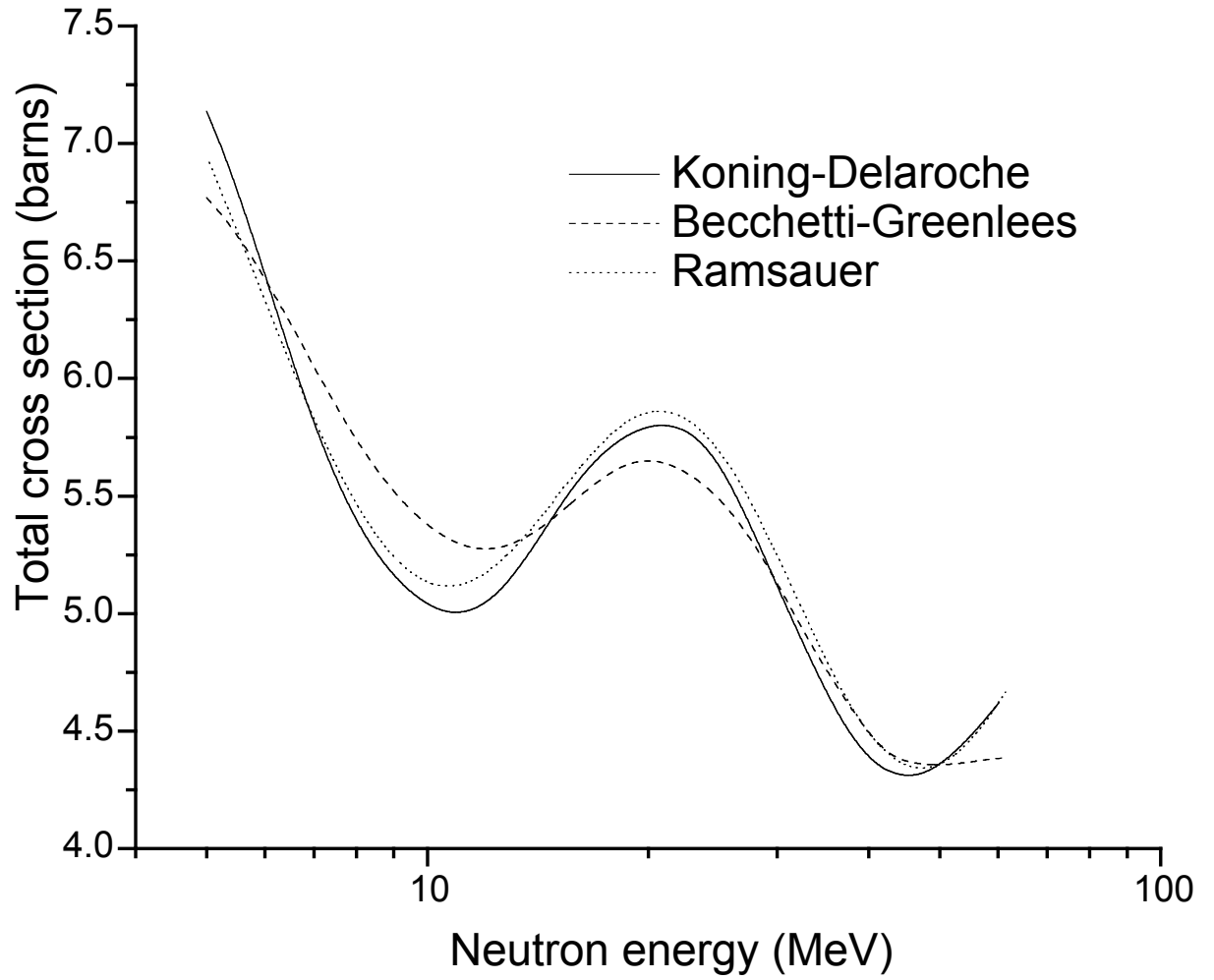


Fig. 1. Different model fits to total cross section data for $n+^{208}\text{Pb}$.

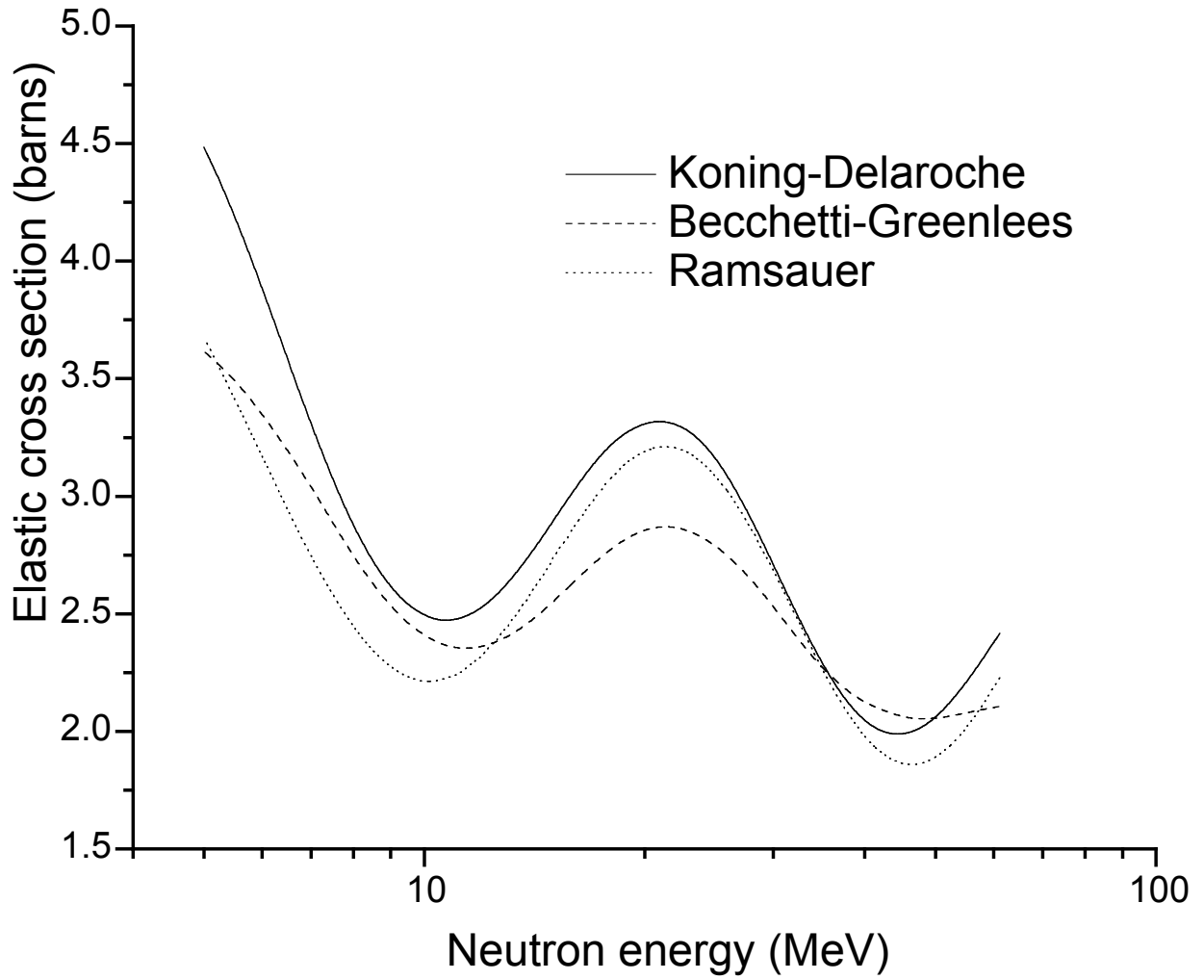


Fig. 2. Different model fits to elastic cross section data for $n + {}^{208}\text{Pb}$.

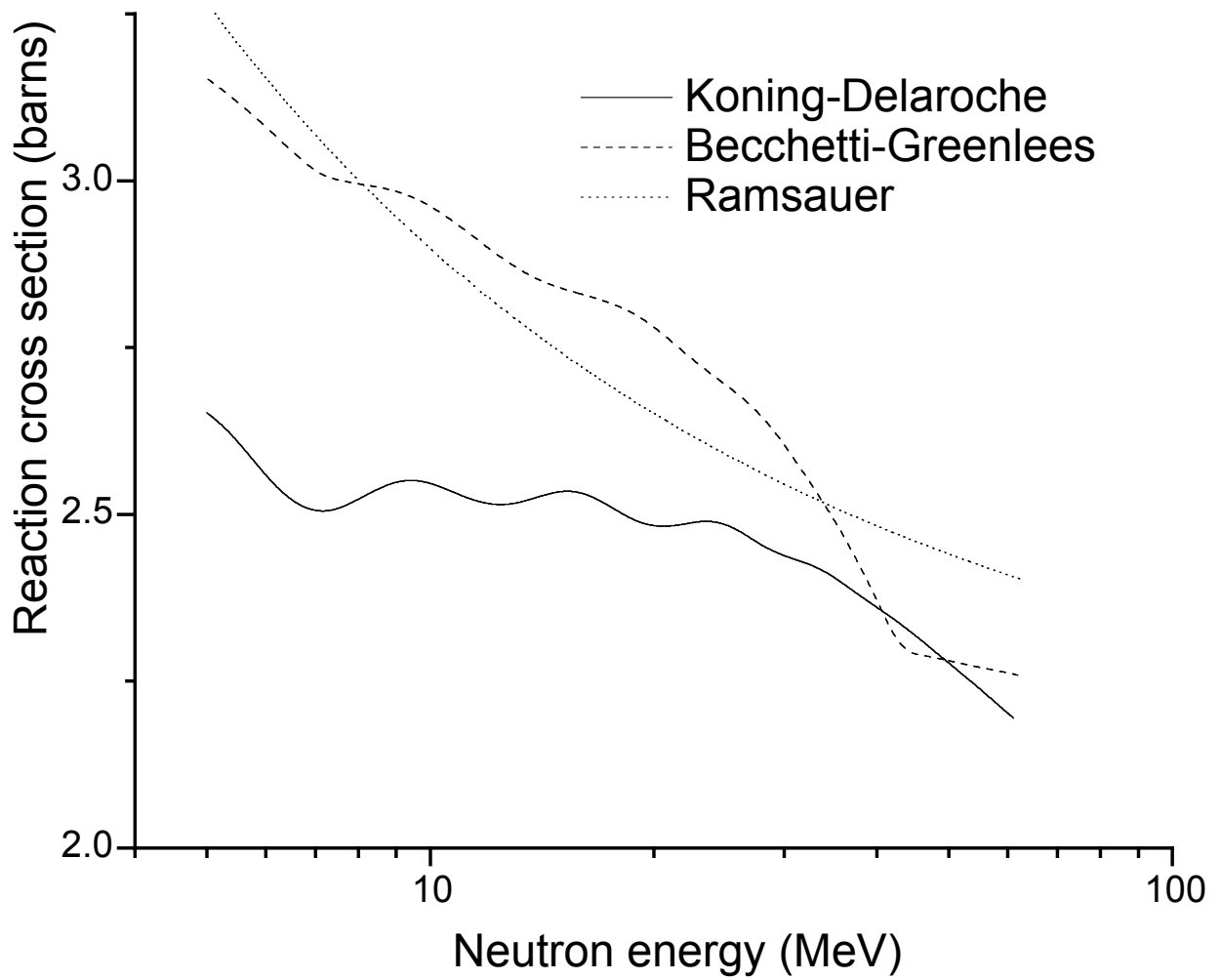


Fig. 3. Different model fits to the reaction (nonelastic) cross section data for $n + {}^{208}\text{Pb}$.

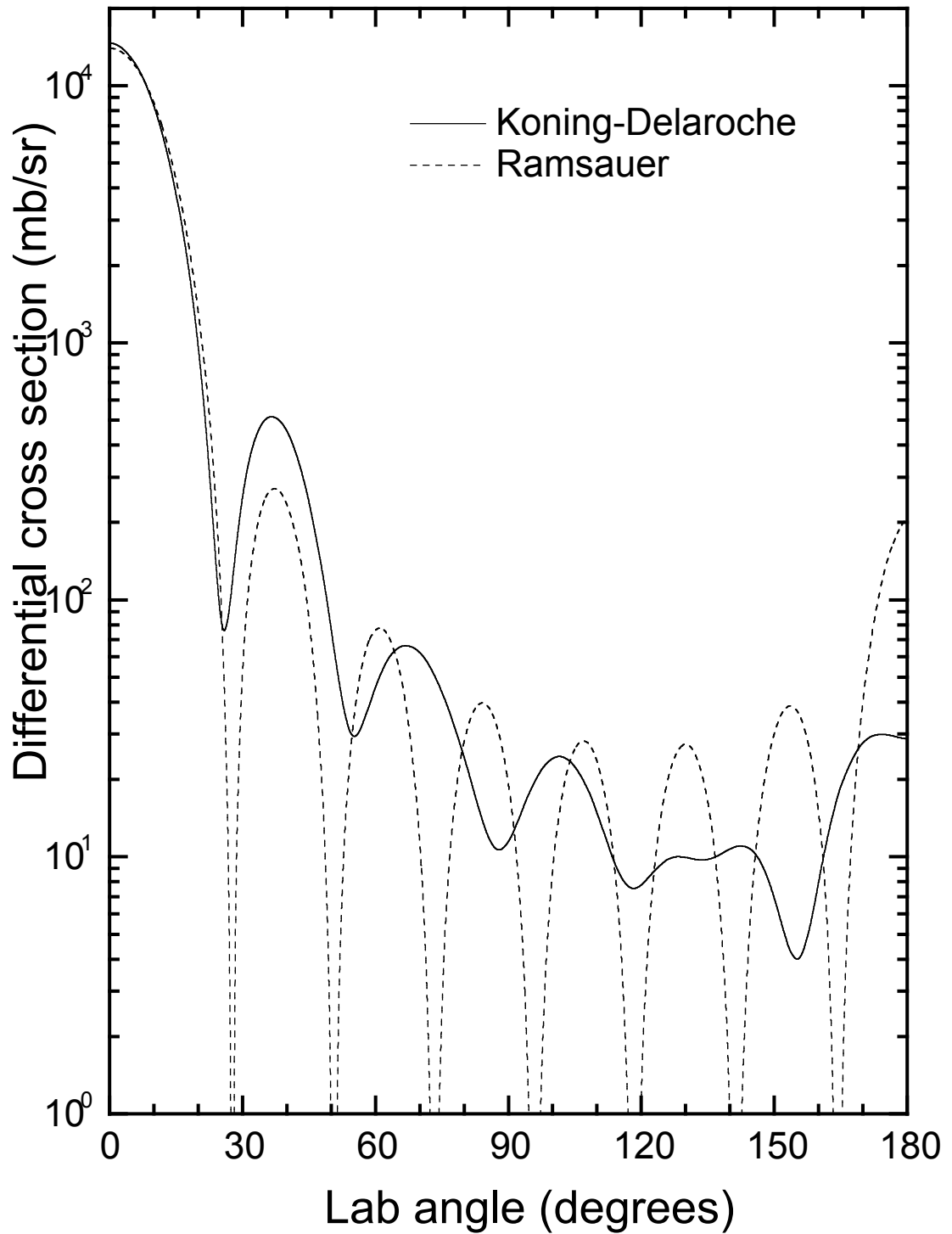


Fig. 4. Angular distributions of elastically scattered neutrons for $E_n = 15.45$ MeV. The Koning and Delaroche optical model is compared with the Ramsauer model for ^{208}Pb .

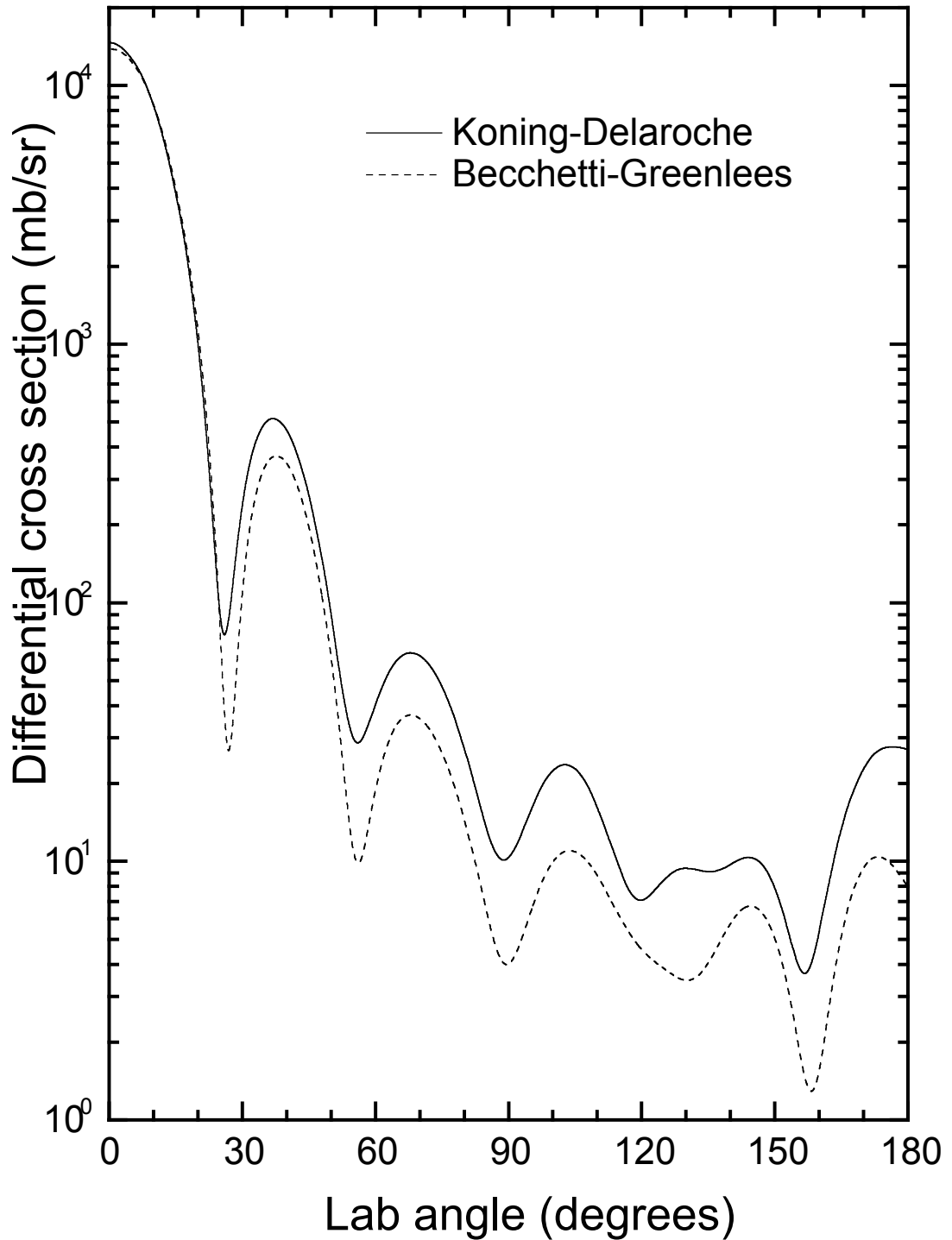


Fig. 5. Angular distributions of elastically scattered neutrons for $E_n = 15.45$ MeV. The Koning and Delaroche optical model is compared with the Becchetti and Greenlees optical model for ^{208}Pb .

IV. Monte Carlo Group Structure

Most neutron Monte Carlo codes (e.g. MCNP¹⁰, COG¹¹, TART¹²) use the “equally-probable-bin” method for sampling scattering angles. The angular distribution tables are a list of $\mu = \cos\theta$ values representing histogram boundaries. The default data tables for these codes have 32 cosine bins, tabulated at a number of incident neutron energies. For an incident neutron energy E falling between tabulated energies E_l and E_h , the distributions for E_l, E_h are randomly chosen with probabilities $P_h = (E - E_l) / (E_h - E_l)$ and $P_l = 1 - P_h$. From the sampled table, a bin is then randomly selected and a cosine value is selected within it with a uniform probability.

The “equally-probable-bin” method tends to smear out fine structure present in the original probability distribution. This smearing effect is markedly apparent in elastic neutron scattering distributions for $E > 5$ MeV. Figures 6-8 show calculated bin densities for the Ramsauer and optical models respectively when $E = 14$ MeV in ^{208}Pb . For 32 bins, the two models yield practically identical bin boundaries. The fine details of the distributions become visible only by significantly increasing the number of “equally-probable-bins.”

The angular distributions of both Ramsauer and optical models are dominated by a pronounced peak in the forward direction. We compared the predicted amounts of forward scattering by running a Monte Carlo simulation and estimating the scattering cone size with respect to the forward direction. Fig. 9 shows the closely matching predictions of the K&D and Ramsauer models as a function of energy.

The “equally-probable-bin” method is extremely fast but at the expense of accuracy. Much of the detail of the original distribution is lost by the necessary assumption of uniform likelihood within each bin. The sampling accuracy could be improved readily by increasing the number of bins, but at the expense of more computer memory. Alternatively, the table lookup technique could be used. This method searches a table of increasing cumulative probabilities until the interval, j , is found within which a given random number, μ , falls. By a judicious choice of the step positions, this method retains the details of the original distribution with a relatively small number of points. A disadvantage of the method is the added computer time required for the table search, and the need for recoding. A fast but less well-known alternative to table lookup is the alias method.¹⁷ It requires two pre-calculated alias probability tables, thereby eliminating the need for a table search. A disadvantage of this technique would be a somewhat larger coding effort.

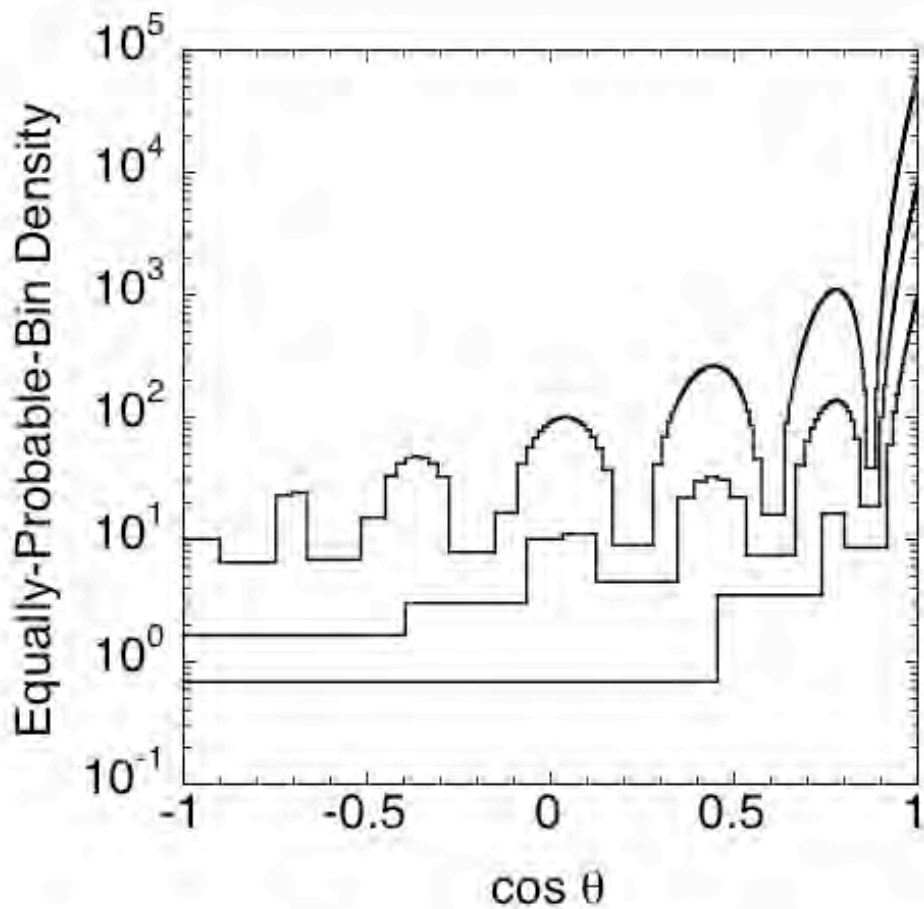


Fig. 6. “Equally-probable-bin” densities for Ramsauer model of ^{208}Pb at neutron energy $E = 14$ MeV. The bin numbers are (from top to bottom) 2048, 256, and 32 respectively.

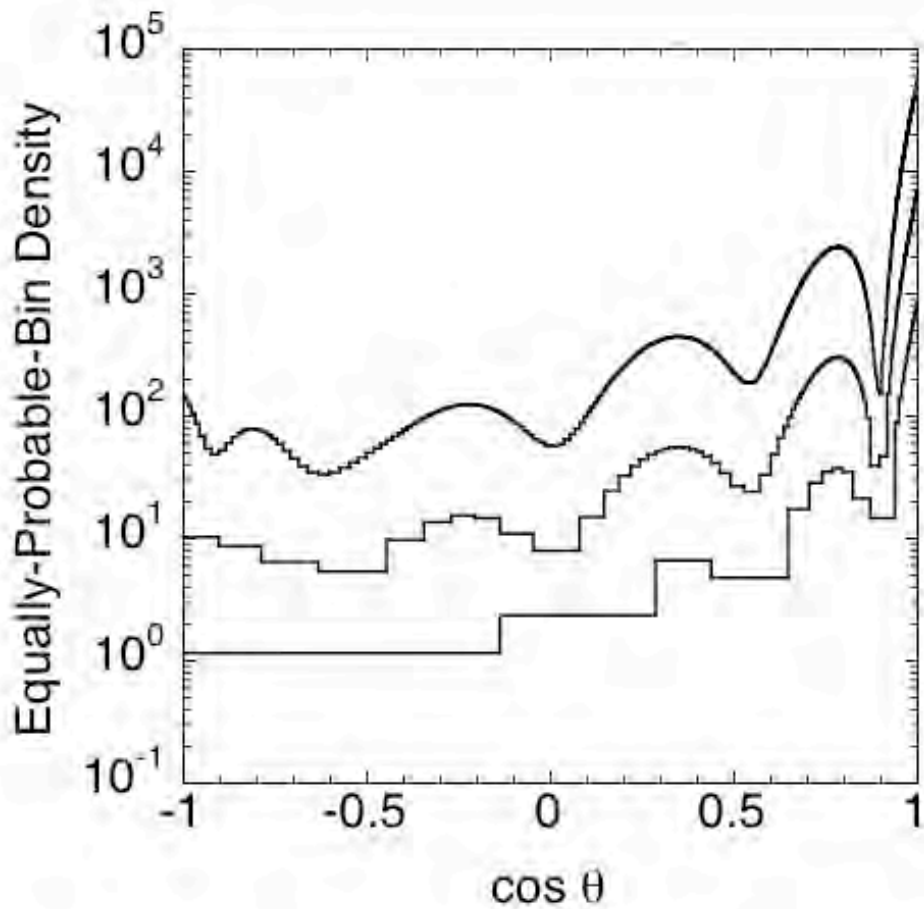


Fig. 7. ‘Equally-probable-bin’ densities for the Koning and Delaroche optical model of ^{208}Pb at neutron energy $E = 14$ MeV. The bin numbers are (from top to bottom) 2048, 256, and 32 respectively.

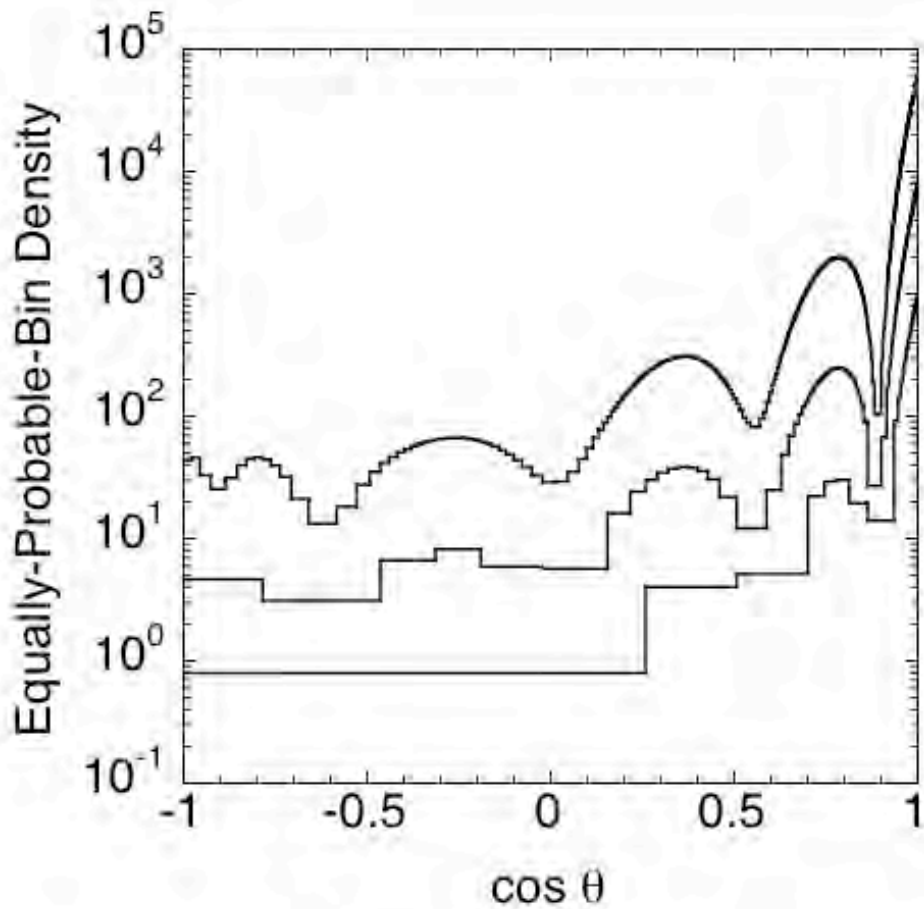


Fig. 8 ‘Equally-probable-bin’ densities for the Becchetti and Greenlees optical model of ^{208}Pb at neutron energy $E = 14$ MeV. The bin numbers are (from top to bottom) 2048, 256, and 32 respectively.

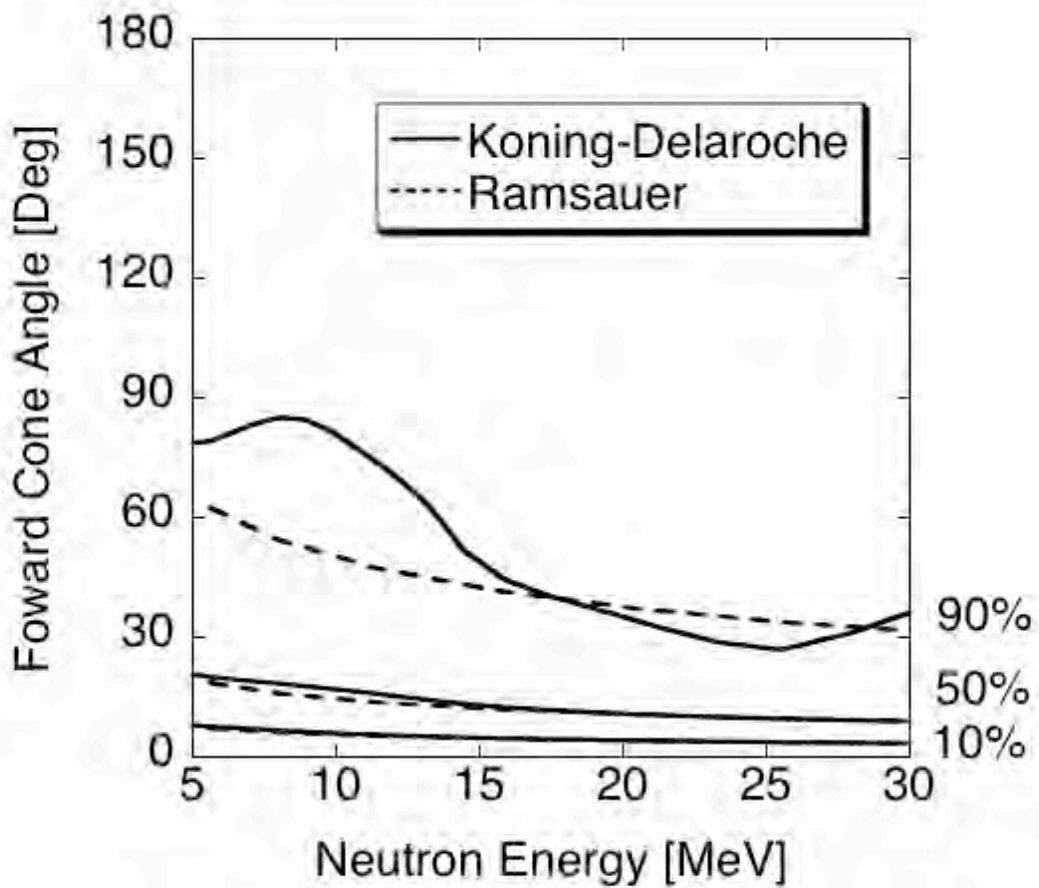


Fig. 9. Elastic scattering forward cone opening angles for Ramsauer (dashed) and Koning and Delaroche optical (solid) models based on 32 equally probable bins. The angles plotted are for 10%, 50%, and 90% of the total neutron scattering probability of ^{208}Pb at neutron energy $E = 14$ MeV.

We have performed several calculations to compare the effect of the angular distribution data on a simple penetration problem. In Table 1 the transmissivity of an infinite slab for neutrons ($E_n = 14$ MeV) at normal incidence is tabulated for slab thicknesses. Each value was obtained using the Monte Carlo method and averaging over 10^7 histories. Table 2 lists the theoretical cross sections employed for sampling the mean free path and reaction. The “equally-probable-bin” technique was used to sample the angular deflection for elastic scattering.

The transport quantity of main interest, the effective scattering cosine, can be defined as

$$\bar{\mu}_{eff} = \frac{1}{2N_{EP}} \sum_i^{N_{EP}} (1 + \bar{\mu}_i) \quad (1)$$

Here N_{EP} is the number of equally-probable-bins, and $\bar{\mu}_i$ is the average scattering cosine of bin i . In Table 3, $\bar{\mu}_{eff}$ of neutrons for the B&G, K&D, and Ramsauer models is given. The value of the effective scattering angle has typically converged to 1% at $N_{EP} = 512$ bins, though in some other nuclei and energies not shown here we occasionally found examples where convergence required 2048 bins.

In all cases shown in Table 1 or Table 3, the Ramsauer model is preferable to an out-of-date optical model fit to the data.

Table 1: Transmissivity through Slab for $E_n=14$ MeV for several slab thicknesses given in units of number of ^{208}Pb atoms per unit area.

	$10^{22} / \text{cm}^2$	$10^{23} / \text{cm}^2$	$10^{24} / \text{cm}^2$
Ram 32-bin	0.9722(3)	0.7524(2)	0.04949(6)
Ram 2048-bin	0.9724(3)	0.7540(2)	0.05011(6)
KD 32-bin	0.9738(3)	0.7613(2)	0.04782(6)
KD 2048-bin	0.9739(3)	0.7622(2)	0.04814(6)
BG 32-bin	0.9716(3)	0.7435(2)	0.04080(6)
BG 2048-bin	0.9713(3)	0.7442(2)	0.04115(6)

Table 2: Cross Sections at $E_n = 14$ MeV [$b = 10^{-24}$ cm²].

	Total [b]	Absorption [b]	Elastic [b]
Ram	5.377	2.757	2.620
KD	5.289	2.526	2.763
BG	5.340	2.847	2.493

Table 3: Effective scattering cosines, μ_{eff} , as a function of the number of equally-probable bins, N_{EP} , is tabulated for different models and energies.

N_{EP}	10 MeV			20 MeV			30 MeV		
	Ram	K&D	B&G	Ram	K&D	B&G	Ram	K&D	B&G
4	0.1407	0.1675	0.1411	0.1348	0.1330	0.1320	0.1312	0.1315	0.1301
8	0.0948	0.1351	0.0953	0.0832	0.0777	0.0722	0.0756	0.0702	0.0692
16	0.0809	0.1213	0.0822	0.0641	0.0513	0.0458	0.0528	0.0494	0.0462
32	0.0787	0.1203	0.0760	0.0620	0.0437	0.0363	0.0481	0.0409	0.0363
64	0.0786	0.1202	0.0748	0.0623	0.0415	0.0332	0.0484	0.0375	0.0327
128	0.0790	0.1201	0.0745	0.0618	0.0408	0.0319	0.0487	0.0364	0.0315
256	0.0789	0.1201	0.0745	0.0621	0.0405	0.0316	0.0489	0.0360	0.0310
512	0.0789	0.1201	0.0745	0.0621	0.0405	0.0316	0.0488	0.0359	0.0309

V. Conclusions

For many applications of transport calculations, such as deep penetration through radiation shielding, the most important quantities are average elastic scattering properties, neutron removal and energy deposits. We have demonstrated that the Ramsauer model is reasonably accurate at describing these features. Given its simplicity, the Ramsauer model may be useful in fast neutron applications for calculating differential elastic scattering distributions and reproducing the magnitude of integrated total, elastic, and reaction cross sections.

For applications where precision on the order of 1% or better is required, we have demonstrated that more careful attention must be paid to (1) accurately representing the relative magnitudes of the elastic and reaction cross sections and (2) improving the resolution of scattering angles over the current 32 equally-probable-bin method.

This work was performed under the auspices of the U.S. Department of Energy by the UC, Lawrence Livermore National Laboratory under Contract No. W-7405-ENG-48.

Appendix

To understand the depth of the minima in angular distributions, we begin with the plane-wave Born approximation (PWBA) for elastic scattering from a real central potential. In this model, as in the Ramsauer model, there are deep minima for which the cross section vanishes. However, these deep minima are absent in realistic optical model calculations. Three features of optical model calculations that lead to less deep minima in the angular distributions than are present in the PWBA are (1) the use of distorted waves instead of plane waves, (2) an imaginary potential which has a different form factor from the real potential, and (3) the spin-orbit interaction which leads to different form factors for neutron parallel and anti-parallel couplings of the neutron spin and orbital angular momentum vectors. Of these three effects, the correct use of distorted waves plays the most significant role in removing the deep minima and in making the diffraction pattern more irregular. Distorted waves are inherent in the Ramsauer-model assumption of a single phase shift for all partial waves – refraction effects have been shown to result in the usefulness of this approximation for incident neutron energies in the range $5 < E_n < 60$ MeV in Ref. 5. However, the correct effect of distorted waves on the angular distribution of elastically scattered neutrons is not included in the Ramsauer model, nor would such an extension be sensible.

One simple extension to the Ramsauer model that removes the deep minima is to account for the above-mentioned effects by introducing a second term with a different radius that adds incoherently to the first. We note here how one of the effects, the spin-orbit potential, leads to two incoherent terms in a realistic optical-model calculation. Unlike the central potential, the spin-orbit potential can flip the spin of the projectile. The differential cross section is the *incoherent* sum of two amplitudes: the non-spin-flip amplitude and the spin-flip amplitude. These amplitudes are incoherent because they lead to final states that are distinguishable.

In such a two-radii Ramsauer model, Eq. (6) for σ would have 2 terms, one term where $R \approx R + \Delta R$ and another term where $R \approx R - \Delta R$. These two terms have minima at different angles and when added together result in shallower minima. For example, in Fig. 10 we show the relative differential cross section that results in this model for $n + {}^{208}\text{Pb}$ at $E_n = 14$ MeV for $\Delta R/R = 0.1$. While the addition of a new parameter, $\Delta R/R$, would lead to a somewhat better representation of the angular distribution of the elastically scattered neutrons, it would not be able to faithfully reproduce the irregularities in the angular distribution (*i.e.*, the spacing of the maxima and minima) which arise due to distortion effects.

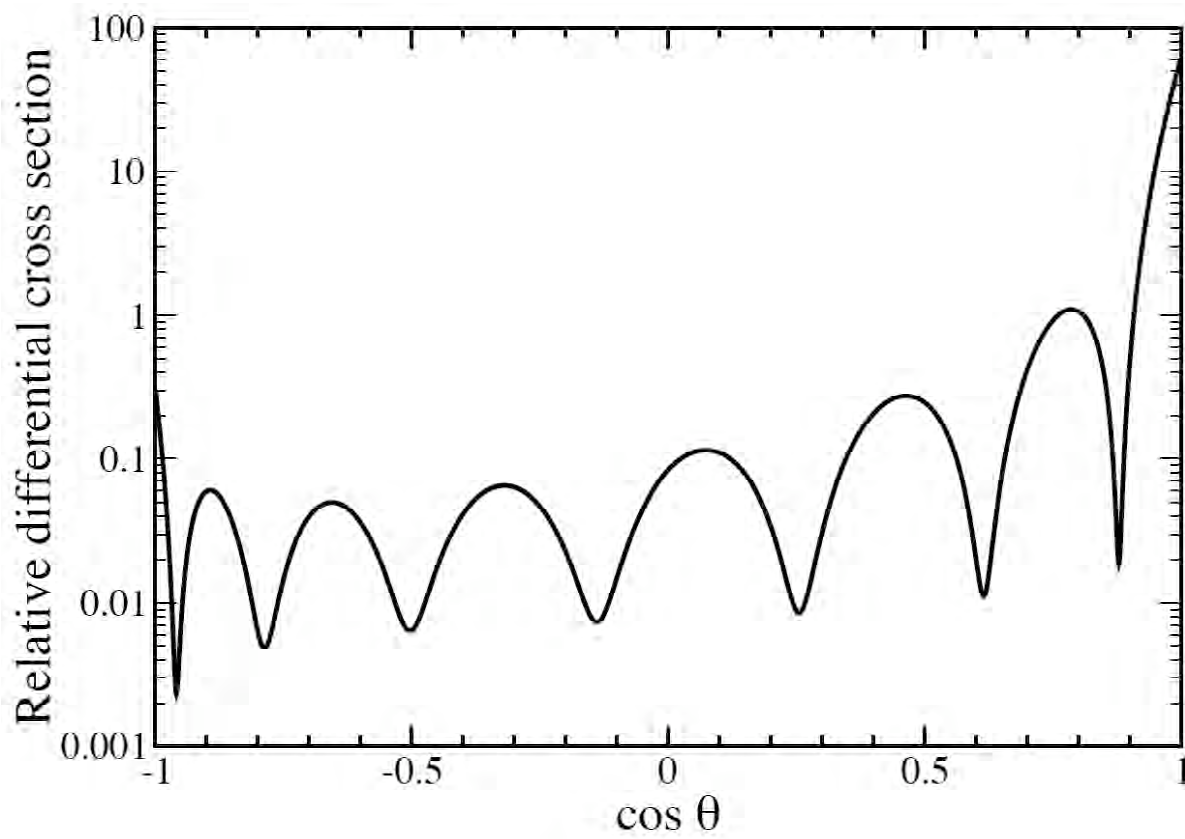


Fig. 10. The relative differential shape-elastic cross section is shown for a two-radii Ramsauer model, resulting in shallower minima.

References

1. J. D. LAWSON, "A Diffraction Effect Illustrating the Transparency of Nuclei to High Energy Neutrons," *Phil. Mag.*, 44, 102 (1953).
2. J. M. PETERSON, "Neutron Giant Resonances – Nuclear Ramsauer Effect," *Phys. Rev.*, 125, 955 (1962).
3. H. S. CAMARDA, T. W. PHILLIPS and R. M. WHITE, "Neutron Absolute and Total Cross Section Difference Measurements in the Mass 140 Region," *Phys. Rev. C*, 29, 2106 (1984).
4. J. D. ANDERSON and S. M. GRIMES, "Nuclear Ramsauer Effect and the Isovector Potential," *Phys. Rev. C*, 41, 2904 (1990).
5. S. M. GRIMES, J. D. ANDERSON, R. W. BAUER and V. A. MADSEN, "Justification of a Simple Ramsauer Model for Neutron Total Cross Sections," *Nucl. Sci. Eng.*, 130, 340 (1998).
6. V. FRANCO, "Quantitative Aspects of Neutron – Nuclear Interaction and the Optical Model," *Phys. Rev. B*, 140, 1501 (1965).
7. R. W. FINLAY, W. P. ABFALTERER, G. FINK, E. MONTEI, T. ADAMI, P. W. LISOWSKI, G. L. MORGAN, and R. C. HAIGHT, "Neutron total cross sections at intermediate energies," *Phys. Rev. C*, 47, 237 (1993); W. P. ABFALTERER, F. B. BATEMAN, F. S. DIETRICH, R. W. FINLAY, R. C. HAIGHT, and G. L. MORGAN, "Measurement of neutron total cross sections up to 560 MeV," *Phys. Rev. C*, 63, 044608 (2001).
8. R. W. BAUER, J. D. ANDERSON, S. M. GRIMES, D. A. KNAPP and V. A. MADSEN, "Application of the Simple Ramsauer Model for Neutron Total Cross Sections," *Nucl. Sci. Eng.*, 130, 348 (1998).
9. MOFAZZAL AZAM and RAJESH G. GOWDA, "Scattering of Intermediate Neutrons from Nuclei and the Ramsauer Hypothesis," *Nucl. Sci. Eng.*, 144, 86 (2003).

10. J.F. BRIESMEISTER (Ed.), "MCNP - A General Monte Carlo N-Particle Transport Code, Version 4B," Los Alamos National Laboratory Report LA-12625-M, Los Alamos, NM (1997).
11. T.R. WILCOX and E.M. LENT, "COG - A Particle Transport Code Designed to Solve the Boltzmann Equation for Deep-Penetration (Shielding) Problems," Lawrence Livermore National Laboratory Report M-221, Livermore, CA (1989).
12. D.E. CULLEN, "Users Manual for TART 2002: A Coupled Neutron-Photon 3-D, Combinatorial Geometry Time Dependent Monte Carlo Transport Code," Lawrence Livermore National Laboratory Report UCRL-ID-126455-REV-4, Livermore, CA (2003).
13. H. S. CAMARDA, Personal Communication (1998)
14. F. S. DIETRICH, J. D. ANDERSON, R. W. BAUER, and S. M. GRIMES, "Wick's Limit and a New Method for Estimating Neutron Reaction Cross Sections," *Phys. Rev. C*, 68, 064608 (2003).
15. A. J. KONING and J.-P. DELAROCHE, "Local and global nucleon optical models from 1 keV to 200 MeV", *Nucl. Phys. A*, 713, 231 (2003).
16. F. D. BECCHETTI and G. W. GREENLEES, "Nucleon-Nucleus Optical-Model Parameters, $A > 40$, $E < 50$ MeV," *Phys. Rev.*, 182, 1190 (1969).
17. A.J. WALKER, "An Efficient Method for Generating Discrete Random Variables with General Distributions," *ACM Trans.Math. Software*, 3(3), 253-256 (1977).